

Optical emission from massive donors in ULX binary systems

Alessandro Patruno¹ & Luca Zampieri²

¹*Astronomical Institute ‘A. Pannekoek’, University of Amsterdam, Kruislaan 403, Amsterdam, The Netherlands: apatruno@science.uva.nl*

²*INAF - Osservatorio Astronomico di Padova, Vicolo dell’osservatorio 5, 35122 Padova, Italy : luca.zampieri@oapd.inaf.it*

2 November 2018

ABSTRACT

We present evolutionary tracks of binary systems with high mass companion stars and stellar-through-intermediate mass BHs. Using Eggleton’s stellar evolution code, we compute the luminosity produced by accretion from the donor during its entire evolution. We compute also the evolution of the optical spectrum of the binary system taking the disc contribution and irradiation effects into account. The calculations presented here can be used to constrain the properties of the donor stars in Ultra-luminous X-ray Sources by comparing their position on the HR or color-magnitude diagrams with the evolutionary tracks of massive BH binaries. This approach may actually provide interesting clues also on the properties of the binary system itself, including the BH mass. We found that, on the basis of their position on the color-magnitude diagram, some of the candidate counterparts considered can be ruled out and more stringent constraints can be applied to the donor masses.

Key words: galaxies: M81, NGC1313, NGC4559, Holmberg II — X-rays: binaries — X-rays: galaxies

1 INTRODUCTION

Point like off nuclear X-ray sources with luminosities well in excess of the Eddington limit for a stellar mass black hole, have been discovered in a large number of nearby galaxies (e.g. Colbert & Ptak 2002; Swartz et al. 2004; Liu & Bregman 2005). These Ultraluminous X-ray Sources (ULXs) are too dim to be low luminosity AGNs and too bright to be normal X-ray binaries (XRBs) emitting below the Eddington limit. In this paper we define a ULX as a source with bolometric luminosity in excess of the Eddington limit for a stellar mass black hole of $20M_{\odot}$ and less luminous than a few 10^{41} erg/s. This definition implies that a Galactic XRB radiating isotropically at or below the Eddington limit can not be a ULX.

In spiral or starburst galaxies ULXs turn out to be associated with star forming regions, emission nebulae and stellar clusters (Zezas et al. 2002, Pakull & Mirioni 2002). These facts along with, in some case, the detection of stellar optical counterparts (Roberts et al. 2001; Goad et al. 2002; Liu et al. 2002; Liu et al. 2004; Kaaret, Ward & Zezas 2004; Zampieri et al. 2004; Kaaret 2005; Mucciarelli et al. 2005; Mucciarelli et al. 2007; Soria et al. 2005) strongly indicate an association between ULXs and young massive stars, although the nature of the accreting compact object remains unclear.

A certain number of ULXs, however, appear as isolated X-ray sources with no obvious counterpart at any wave-

length (Soria & Motch 2004) and without a clear association with star forming regions or emission nebulae. Some low-luminosity ULXs may possibly be present also in elliptical galaxies (Jeltema et al. 2003), but their nature and the actual evidence for their existence is not well established (see e.g. Irwin, Bregman & Athey 2004, Arp, Gutiérrez & López-Corredoira 2004, Gutiérrez & López-Corredoira 2005).

The nature of the ULXs in spiral galaxies is less controversial. Different models have been proposed to explain the large luminosities reached by these sources. One of the favored models consists of an intermediate mass black hole (IMBH) with a mass in the range $10^2 - 10^3 M_{\odot}$, accreting from an high mass donor star. The presence of an IMBH can account for most of the observational properties of ULXs in a rather straightforward way. For instance, the observed cool disc spectra of some ULX can be explained with the fact that the innermost stable circular orbit of an IMBH is larger than that of a stellar mass black hole (e.g. Miller, Fabian Miller 2004). The detection of a ~ 50 -160 mHz quasi periodic oscillations in the power density spectrum of M82 X-1 and NGC5408 X-1 (Strohmayer & Mushotzky 2003, Fiorito & Titarchuk 2004, Mucciarelli et al. 2006; Strohmayer et al. 2007), the very high luminosity of some ULXs ($\sim 10^{41}$ ergs $^{-1}$) along with their cool discs, and the energy content and morphology of the nebulae around some of them (Pakull & Mirioni 2002) all suggest an IMBH inter-

pretation. The main problem with this interpretation resides in the formation mechanism of such an extreme object. In fact, if IMBHs with masses in excess of $\sim 100M_{\odot}$ exist, they will require a new formation root with respect to the stellar black holes in our Galaxy and to the supermassive black holes in Active Galactic Nuclei. Until now two scenarios have been proposed to form a black hole in the intermediate mass range: the runaway collision of massive stars in dense open clusters (Portegies Zwart et al. 2004, Gürkan et al. 2004) and the primordial collapse of a very high mass star with zero metallicity (Abel et al. 2000, Madau & Rees 2001). Both the mechanisms however suffer of a certain degree of uncertainty related to the incomplete knowledge of the behavior of very massive stars. Therefore we have no final evidence that an IMBH can really form. Furthermore, the interpretation of the soft components observed in some ULXs in terms of cool accretion discs is not univocal (e.g. Clark et al. 2005, Dewangan et al. 2005, Roberts et al. 2005, Feng & Kaaret 2006, Gonçalves & Soria 2006, Stobbart et al. 2006).

Other interpretations in terms of stellar (or quasi-stellar) mass black holes have been proposed. A mechanical (King et al. 2001) or a relativistic beaming (Körding, Falcke & Markoff 2002) can reproduce the observed luminosities of ULXs up to a few $10^{40} \text{ erg s}^{-1}$ with a beaming factor around ~ 10 . At most, as suggested by King & Dehnen 2005, accretion from helium rich matter from a geometrically thick disc can generate luminosities up to $\sim 5 \times 10^{40} \text{ erg s}^{-1}$. However, luminosities in excess of $5 \times 10^{40} \text{ erg s}^{-1}$ ($\sim 5\%$ of the ULX population) and the isotropy of the ionized nebulae around some ULXs can not be easily explained in terms of beaming models. On the other hand, photon bubbles disc instabilities (Begelman 2002, Begelman 2006) and emission from a slim disc (Watarai, Mizuno & Mineshige 2001, Ebisawa et al. 2003) can produce genuine isotropic super-Eddington luminosities around 10 times the Eddington limit.

As shown by Rappaport et al. (2005), a normal binary with a stellar mass black hole and a donor star with initial mass $\gtrsim 10M_{\odot}$, can in principle explain a large sample of ULXs if a super Eddington luminosity around 10 is allowed (see also Podsiadlowski et al. 2003). However, the typical temperature of a slim disc in this regime ($\sim 1\text{--}2 \text{ keV}$) is inconsistent with the observation of some cool disc sources which are, at the same time, the most luminous ULXs. Furthermore, luminosities in excess of a few $10^{40} \text{ erg s}^{-1}$ are not attainable with slim discs around stellar mass black holes. On the other hand, the photon bubble instability model makes no predictions on the observable accretion disc temperature and therefore cannot be compared directly with observations.

Thanks to the high precision astrometry of the *Chandra* X-ray observatory, we know that some ULXs have optical counterparts which match with the X-ray source position (Liu et al. 2002, Liu et al. 2004, Zampieri et al. 2004, Kaaret, Ward & Zezas 2004, Soria & Motch 2004, Kaaret 2005, Mucciarelli et al. 2005; Mucciarelli et al. 2007, Liu et al. 2007). Most of them are suspected to be main sequence (MS) high mass stars or supergiant stars of uncertain spectral type. The ambiguity arises because, until now, optical spectra of these stars either are not available, or they are too noisy and with peculiar spectral features (Liu et al. 2004), or there is more than an optical counterpart in the X-ray error box (Soria & Motch 2004, Mucciarelli et al. 2005).

In this paper, we present the evolutionary tracks of binary systems with high mass companion stars and stellar-through-intermediate mass BHs and compare them with the properties of the donor stars in ULX binary systems. In §2 we present the model adopted to evolve the binary system. In §3, we summarize the properties of the four ULXs considered and their optical counterparts. Our results are presented in §4 and compared with the properties of ULX counterparts in §5. Conclusions follow in §6.

2 MODEL

We consider a binary system with a stellar mass BH ($10 M_{\odot}$) or an IMBH ($\gtrsim 100M_{\odot}$) and a companion star that is orbiting around it and eventually transferring matter onto it. The evolution of the binary is computed using an updated version of the Eggleton code (Eggleton 1971; Pols et al. 1995). The calculation follows that presented in Patruno et al. (2005). We assume a Population I chemical composition ($Y=0.28, Z=0.02$) and allow for non-conservative stellar evolution, taking into account wind loss from luminous stars (de Jager et al. 1988). The adopted mixing length parameter and overshooting constant are $\alpha = 2.0$ and $\delta_{ov} = 1.2$, respectively (Pols et al. 1998). Loss of angular momentum is also accounted for through emission of gravitational waves (see e.g. Landau & Lifshitz 1975) and particles in winds (Soberman, Phinney & van den Heuvel 1997).

If accretion occurs via Roche-lobe overflow (RLOF), we assume that an accretion disc will form. In this work we adopt an efficiency $\eta = 0.1$ for the conversion of gravitational potential energy into radiation in a disc. The bolometric luminosity of the X-ray source is $L = \eta \dot{M} c^2$, where \dot{M} denotes the average mass transfer rate from the donor as computed from the numerical code.

In case accretion occurs via mass loss from a stellar wind (wind-fed accretion; WFA), the situation is somewhat different if one considers stellar mass BHs or IMBHs, as the latter are bigger and have a stronger gravitational potential well. Hence, owing to the larger gravitational capture radius, a comparatively larger fraction of the wind emitted by the donor star can be captured at corresponding orbital separations. Furthermore, a large fraction of the accreting particles have a significant orbital angular momentum. This might be sufficient to form an accretion disc even in a wind-fed system with a IMBH, although further investigations are required to completely understand the geometry of these discs. In the following we will limit our analysis only to WFA systems with IMBHs. For the WFA model we adopt a modified version of the RLOF model, adding an equation to compute the WFA accretion rate (as described in Patruno et al. 2005). An accretion disc is assumed to form also in this case but, unless the donor is very massive ($\gtrsim 60M_{\odot}$, not considered in this work), the accretion rate is essentially negligible.

2.1 Initial orbital separation

The evolution of a binary system containing a BH/IMBH depends on the initial orbital separation. The companion star can fall in three different zones, defined in terms of the zero-age/terminal-age main sequence (ZAMS/TAMS) radius of the donor R_{ZAMS}/R_{TAMS} , the tidal radius of the system

R_T and the Roche lobe radius of the companion R_L . The expressions of these radii are (Eggleton 1983, Demircan & Kahraman 1991):

$$R_{ZAMS} = \left(\frac{M}{M_\odot}\right)^{0.57} R_\odot \quad (1)$$

$$R_{TAMS} = 1.6 \left(\frac{M}{M_\odot}\right)^{0.83} R_\odot \quad (2)$$

$$R_T = \left(\frac{M_{BH}}{M}\right)^{1/3} R \quad (3)$$

$$R_L = \frac{0.49q^{2/3}a}{0.6q^{2/3} + \ln(1 + q^{1/3})}, \quad (4)$$

where M and R refer to the donor star, M_{BH} is the black hole mass, $q = M/M_{BH}$ is the mass ratio, and a is the orbital separation.

In a reference frame centered on the BH/IMBH, the **first zone** lies between $a = 0$ and $a \sim R_T$. If the companion star enters in the first zone, it is disrupted by the strong tidal forces of the BH, likely resulting in an outburst of short duration (Rees 1988, Ulmer 1999, Ayal, Livio & Piran 2000). This possibility is not considered in the present work.

The **second zone** is defined as the interval of orbital separations where the stellar surface can reach contact with the Roche lobe radius R_L sometime during MS. In the following we will refer to the binaries whose donor falls in the second zone as “case A” systems. In order for the initial orbital separation to be in this range, either the companion star is tidally captured by the BH/IMBH (Hopman, Portegies Zwart & Alexander 2004, Baumgardt et al. 2006) or the binary system undergoes an exchange interaction with another star (Baumgardt et al. 2004, Alexander & Livio 2004, Blecha et al. 2006).

If the initial orbital separation a is such that $R_L > R_{TAMS}$, the companion is in the **third zone**. In this zone, mass transfer occurs through RLOF only when the donor is in the H-shell phase (case B) or during the He-shell burning (case C). If the star falls in this zone, during the main sequence the only possible accretion mechanism is the gravitational capture of wind particles. WFA IMBHs systems can reach ULX luminosities even if the orbital separation is a few astronomical units, thanks to the enhanced gravitational focusing effect of the IMBH. However, for larger separations, the source is fainter and has a mean luminosity typical of bright Galactic XRBs (see Patruno et al. 2005 for an extended discussion). If the initial separation is very large (usually several tens of astronomical units), neither RLOF nor WFA are possible, and the system evolves essentially as a detached, non-interacting binary.

2.2 Stability of the accretion disc around an IMBH

The accretion disc around a BH is steadily fueled if the mass transfer rate from the donor exceeds the critical mass transfer rate (Dubus et al. 1999):

$$\dot{M}_{cr} = 2.4 \cdot 10^{-6} \left(\frac{M_{BH}}{10^2 M_\odot}\right)^{1/2} \left(\frac{M}{15M_\odot}\right)^{-0.2}$$

$$\times \left(\frac{M_{BH} + M}{10^2 M_\odot}\right)^{-0.7} \left(\frac{a}{1 \text{ AU}}\right)^{2.1} M_\odot \text{ yr}^{-1} \quad (5)$$

The critical mass accretion rate given above takes already into account the stabilizing effect of the increase in temperature due to the disc self-irradiation. In our model, all the IMBH systems accreting through RLOF turn out to be persistent if the donor mass is higher than $\sim 10M_\odot$, in agreement with the findings of Portegies Zwart, Dewi & Maccarone (2004) and Patruno et al. (2005). For a stellar mass BH the stability of the disc is guaranteed down to donor masses $\sim 5M_\odot$.

Assuming that equation [5] holds also for WFA discs around IMBHs, thermal instabilities are likely to arise. In fact, the mass transfer rate in WFA systems is smaller than that in RLOF systems. All the IMBH WFA systems with a donor star lighter than $30M_\odot$ might experience transient accretion (Patruno et al. 2005). Stars heavier than $30M_\odot$ likely produce a transient phase during the early MS (when the mass transfer rate is small) and a persistent phase during the late MS (when the mass transfer is higher than the critical mass transfer rate). So we expect rapid outbursts and quiescent states (similar to those observed in Galactic transient XRBs) in low mass companion WFA systems and, in general, during the early evolution of WFA systems. The recurrence time and duty cycle are difficult to estimate. As in a dynamical exchange interaction it is highly probable that the companion star falls in the **third zone**, WFA systems might be rather common. Thus, a significant population of IMBH binaries that appear as transient ULXs or even transient XRBs might exist in external galaxies or even in our own galaxy. Some sources of this transient ULX population start to be identified (e.g. Feng & Kaaret 2007).

2.3 X-ray reprocessing in ULXs

An important effect to consider when assessing the properties of ULX counterparts is the possible strong optical-UV contamination caused by the emission of the accretion disc itself and, in case of isotropic emission, also by the reprocessed X-ray radiation. The main reprocessing sites are the outer part of the accretion disc and the donor surface. We follow the evolution of the optical luminosity and colors of the binary system taking irradiation effects into account.

Our calculation relies on the same assumptions discussed in Copperwheat et al. (2005) and Mucciarelli et al. (2007). More specifically, a standard Shakura-Sunyaev disc (e.g. Frank, King & Raine 2002) is assumed and both the X-ray irradiation of the companion and the self-irradiation of the disc are accounted for. However, in order to keep our treatment simple, the companion star is taken to be spherical and at uniform temperature, neglecting the effects produced by the Roche lobe geometry and also those related to the (possible) deformation induced by radiation pressure. We adopt a simplified description of radiative transfer for the interaction of the X-rays with the disc and donor surfaces (a X-ray illuminated plane-parallel atmosphere in radiative equilibrium) and do not include limb and gravity darkening. The shadowing of the disc on the star is continuously monitored during the whole evolution and never overcomes $\sim 15\%$.

The computed luminosity and colors depend on the masses of the donor and BH, the binary period (or orbital separation), the accretion rate and the (unirradiated) temperature of the donor, in addition to the inclination angle i and the orbital phase ϕ that are kept fixed at $\cos i = 1$ (disc face-on) and $\phi = 0$ (superior conjunction). The accretion efficiency and the albedo of the donor surface layers were chosen to be 0.17 and 0.9 respectively. Following Copperwheat et al. (2005), we took the hardness ratio $\xi = F_X(< 1.5 \text{ keV})/F_X(> 1.5 \text{ keV}) = 0.1$. The absorption parameters in the same two spectral bands were selected as $k_s = 2.5$ and $k_h = 0.01$. The R, V and B magnitudes of the (irradiated) disc plus donor have been computed using the output values of the parameters provided by the binary evolution code. In particular, the accretion rate is instantaneously taken to be equal to the mass transfer rate from the companion. When the accretion rate overcomes \dot{M}_{Edd} , we impose $\dot{M} = \dot{M}_{Edd}$ and assume that the excess mass is expelled from the system.

3 ULXS WITH OPTICAL COUNTERPARTS

The purpose of our work is to provide a tool for comparing the observational properties of ULXs with identified optical companions with those predicted for the donors of our BH/IMBH binary model. As reference cases, we consider four ULXs for which sufficient information on the optical counterparts are available to allow a meaningful comparison. They are: NGC1313 X-2 (Miller et al. 2003, Zampieri et al. 2004, Mucciarelli et al. 2005; Mucciarelli et al. 2007, Liu et al. 2007), Holmberg II X-1 (Dewangan et al. 2004, Kaaret, Ward & Zezas 2004), NGC4559 X-7 (Cropper et al. 2004, Soria et al. 2005) and M81 X-9 (Miller, Fabian & Miller 2004). None of the ULXs considered have a unique optical counterpart. In the case of NGC1313 X-2, there are two optical counterparts in the *Chandra* error box, identified on *VLT* and *HST* images. Photometry and modeling of the donor emission are consistent with the following interpretation: an early B MS star of $10\text{--}20M_\odot$ and a red/yellow supergiant of $10M_\odot$ (Mucciarelli et al. 2005, Mucciarelli et al. 2007). For the three other ULXs, only optical photometry is available, and the nature of the donor star is still uncertain.

Fits of the X-ray spectra of these ULXs have been carried out by several authors. Parameters of the best fit obtained with different models are listed in Table 1 and are used to obtain an estimate of the total X-ray luminosity of the system, extrapolating the flux in the energy range $0.05\text{--}20 \text{ keV}$ using the web interface to PIMMS (WebPIMMS v. 3.9c). For M81 X-9 we adopt the bolometric luminosity reported by Miller, Fabian & Miller (2004).

Finally, we briefly summarize the main properties of the optical counterparts of the four ULXs considered in this work. All the spectral classifications and mass estimates reported below are rather uncertain and assume that the donor can be treated as if it were a single star. In addition, except for NGC1313 X-2, contamination of the optical emission from the accretion disc and X-ray irradiation at the donor surface are not accounted for.

- **NGC4559 X-7** (Cropper et al. 2004, Soria et al. 2005): six stars fall inside and two more counterparts are slightly

outside the *Chandra* error box of this ULX. The most luminous is a blue object with properties consistent with a main sequence star of $\sim 20M_\odot$ (Copperwheat et al. 2005). Using color-magnitude diagrams based on the Geneva tracks, Soria et al. (2005) suggest that the colors of the six counterparts inside the error box are consistent with donors with mass between 9 and $25M_\odot$.

- **NGC1313 X-2** (Zampieri et al. 2004, Mucciarelli et al. 2005; Mucciarelli et al. 2007; Liu et al. 2007): two objects, C1 and C2, are present inside the *Chandra* error box of this source having spectral type consistent with an early B MS star of $\sim 10\text{--}18M_\odot$ or a G supergiant of $\sim 10M_\odot$, respectively (Mucciarelli et al. 2005; Mucciarelli et al. 2007). Liu et al. (2007) find that the spectral energy distribution of object C1 is consistent with either a $\sim 8M_\odot$ star of very low metallicity or an O spectral type, solar metallicity star of $\sim 30M_\odot$.

- **Holmberg II X-1** (Dewangan et al. 2004, Kaaret, Ward & Zezas 2004): as other ULXs, this source is embedded in a ionized nebula (Pakull & Mirioni 2002). A star with color $B - V$ and optical magnitude consistent with a O4 – O5V or B3Ib spectral type falls inside the X-ray error box. The corresponding mass is, respectively, $\gtrsim 60M_\odot$ for a MS donor and $\sim 20\text{--}25M_\odot$ for a supergiant.

- **M81 X-9** (Miller, Fabian & Miller 2004): this source is fully embedded in a ionized nebula inside the dwarf companion galaxy of M81, Holmberg IX (Pakull & Mirioni 2002). Inside the X-ray error box there is a blue luminous star with magnitude $B = 22.1$ that, at a distance of 3.4 Mpc , corresponds to an absolute magnitude $B = -5.6$, consistent with a $60M_\odot$ MS star of spectral type O5V or a B2Ib supergiant with mass $\sim 20\text{--}25M_\odot$.

4 INTRINSIC OPTICAL EMISSION FROM MASSIVE DONORS IN BINARIES

In the following we present the evolutionary tracks of binary systems with high mass companion stars and stellar-through-intermediate mass BHs. The results of this computation will be compared with the observed properties of ULX systems in the next Section. The calculation has been carried out adopting the model described in Section 2 and using a modified version of the Eggleton code (Patruno et al. 2005). We focus on the modeled optical properties of massive ($10\text{--}50M_\odot$) donor stars in binaries during mass transfer phases. The accreting black hole masses are in the range $10\text{--}500 M_\odot$. Binaries with less massive donors ($\sim 2\text{--}10M_\odot$) and stellar mass black holes have been investigated by Rappaport et al. (2005), while calculations of the evolutionary tracks for $1\text{--}9M_\odot$ stars accreting onto stellar BHs and IMBHs are presently under way.

As shown by Madhusudhan et al. (2006), who evolved $\sim 10^5$ BH binaries to study the production efficiency of ULX systems, the initial orbital period for triggering a RLOF phase during MS and originating a significantly large population of active ULXs in binaries with massive donors is in the range $\sim 1\text{--}5$ days. We therefore limit our analysis to a selected number of models with initial parameters having the values reported in Table 2. The three groups (A, B and C) are characterized by the different evolutionary phase at which mass transfer sets in (see also §2.1). For Case A, the

Table 1. Spectral parameters and luminosity of the ULXs considered in this work.

ULX	N_H	kT	Γ	L_X	L_{bol}^a	Model ^b	source
	(10^{21}cm^{-2})	(eV)		(10^{39}erg s^{-1})	(10^{39}erg s^{-1})		
NGC1313 X-2	$3.13^{+0.92}_{-0.37}$	200^{+40}_{-50}	$2.23^{+0.15}_{-0.09}$	3.4	7.0	PL+MCD	Zampieri et al. (2004)
Holmberg II X-1	$1.4^{+0.3}_{-0.03}$	128^{+22}_{-13}	$2.40^{+0.07}_{-0.08}$	17	37.7	PL+BB	Dewangan et al. (2004)
NGC4559 X-7	$4.3^{+0.9}_{-1.1}$	120^{+10}_{-10}	$2.23^{+0.06}_{-0.05}$	19	36.9	PL+BB	Cropper et al. (2004)
M81 X-9	2.3	260^{+20}_{-50}	1.73	11	27	PL+MCD	Miller, Fabian & Miller (2004)

^aTotal X-ray (0.05–20 keV) luminosity computed using the web interface to PIMMS (ver. 3.9c).

^bPL=power-law; MCD=multicolor disc blackbody; BB=blackbody

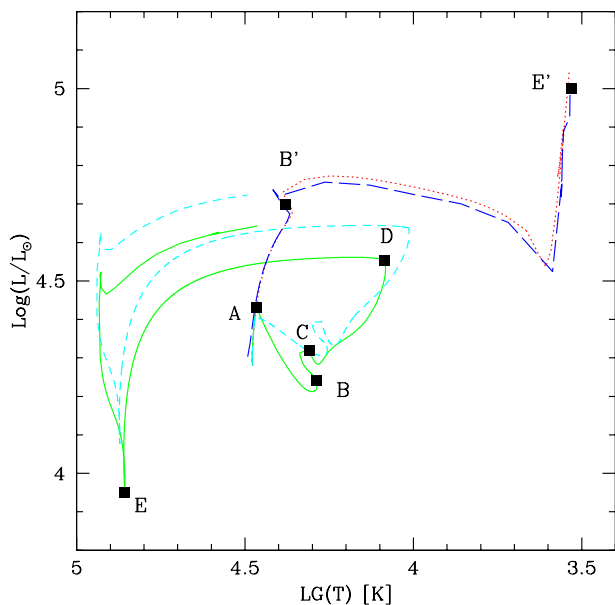


Figure 1. HR diagram for a $15 M_{\odot}$ donor in a binary system with a black hole of 10 and $100 M_{\odot}$ (green-solid and light blue-dashed line) and evolving as a single star (dark blue-long dashed line). The red-dotted line is the Geneva track and has been plotted for comparison. During the binary evolution RLOF sets in during MS (point A) and originates a qualitatively different track caused by the donor losing its envelope onto the BH. Two episodes of mass transfer occur (segments A–B and C–D). The point B' refers to the TAMS and is in the equivalent position of point B in the binary track. In point E and E' the donor ignites the He-core. The tracks end with the He-core ignition for single stars and with the C-core ignition for binary systems.

bolometric luminosity of the system reaches at least 10^{40} – 10^{41} erg s^{-1} (depending on the donor mass) at some stage during MS. For stellar mass BHs, a suitable degree of beaming needs to be invoked in order to reach similar isotropic luminosities.

In Figure 1 we show the evolutionary tracks on the HR diagram of single stars and stars accreting through RLOF in a binary system. As we want to show the differences between the evolution of a single star and that in an accreting binary system, we do not include irradiation. The donor and the single star tracks refers to a $15 M_{\odot}$ star, whereas the accretors are a $10 M_{\odot}$ BH and an IMBH of $100 M_{\odot}$. When RLOF sets in (point A), the track of a star in a binary starts

to diverge from that of a single star. For the models shown in Figure 1, this occurs during MS. The luminosity starts to decrease with time as the decrease in surface temperature is not accompanied by a corresponding increase in radius (which is limited by the Roche lobe). Thus, during MS (segment A–B), a single star is generally more luminous than a star of the same mass in a binary system. The temperature and luminosity of a MS star in a binary system are more similar to those of a less massive star. This may lead to misinterpret a real MS star with one that is crossing the Hertzsprung Gap, causing uncertainties (up to $2 - 5 M_{\odot}$ for a $15 M_{\odot}$ star) in the estimate of the donor mass. The system detaches in point B after an accretion phase of $\sim 10^7$ yrs, very close to the terminal age main sequence.

During the H-shell burning the envelope of the star expands and the binary starts a new episode of mass transfer lasting 10^4 – 10^5 yrs (segment C–D). The system widens because of the large amount of material that is rapidly transferred from the secondary to the BH. As a consequence, the RL increases significantly and, despite the star becomes cooler, the luminosity increases. While during this phase single stars simply move to the right of the HR diagram, becoming progressively colder and undergoing core contraction and envelope expansion (Hertzsprung Gap and Giant branch), stars in binary systems do not cool so much and show a lower luminosity (by a few tenth of magnitude) than single stars of the same mass at a corresponding evolutionary phase. At a certain phase during H-shell burning (point D), all the H envelope is accreted and what is left of the star (the helium core) contracts causing the binary to detach. From point D to carbon core ignition, the donor remains always in a detached phase. At point E the He-core ignites ($L_{He}/L_H > 10$) and the evolution becomes extremely fast with the track stopping after the onset of C-core burning.

Figure 1 shows also the evolutionary track for a donor accreting onto a $100 M_{\odot}$ BH starting the contact phase when the radius of the companion is comparable to the $10 M_{\odot}$ BH case. The overall evolution is similar to the stellar mass BHs, apart from the fact that stars accreting onto an IMBH are more luminous. This is a consequence of the fact that, while the surface temperature remains essentially comparable at a corresponding evolutionary phase, the RL of the donor (and therefore its radius during the contact phase) grows more rapidly in an IMBH binary than in a stellar BH system (see Figure 2).

An important observational diagnostic for stars is represented by the color-magnitude (CM) diagram. The CM diagram of a $15 M_{\odot}$ donor accreting onto a 10 and 100

Table 2. Initial parameters for ULX binary systems. Case A refers to binaries where the donor starts the first Roche lobe contact phase during MS, while case B and C refer to donors starting RLOF during the H-shell or He-shell burning phase, respectively. The first and second columns are the initial donor and accretor masses, while the third column is the initial orbital period of the binary system.

Case	$M(M_{\odot})$	$M_{BH}(M_{\odot})$	Initial P_{orb} (days)
A	10,15,30,50	10,100,500	1-2
B	10,15,30,50	10,100,500	5-15,400-500
C	10,15,30,50	10,100,500	800-1000

M_{\odot} BH is reported in Figure 3 and Figure 4. The tracks calculated for single stars differ in a relevant way with respect to those of a Case A binary that starts mass transfer during MS, as the cold branch that is covered in the CM diagram during the post giant phase is absent. The notation is the same used in the HR diagram. Therefore, the contact phases correspond to the segments A–B (MS) and C–D (H-shell burning). After point D the system detaches and the star turns back on the CM diagram, following backwards the same path crossed during the H-shell contact phase and the MS. This behavior is strictly related to the evolution of the donor after MS discussed above.

Figure 3 and Figure 4 also show how the tracks modify after including the optical emission of the X-ray irradiated accretion disc and donor surface. When mass transfer sets in at point A, the evolution of the irradiated system detaches from the non-irradiated one, as irradiation is enhancing both the observed star luminosity and effective temperature. For a large part of the evolution, at corresponding evolutionary times, the track of the X-ray irradiated system is shifted towards the blue by $\sim 0.1 - 0.2$ magnitudes, while showing a comparable increase in the V magnitude. Only when, close to the end of the second mass transfer episode (point D in Figures 1 and 2), the system is very wide and starts to detach, irradiation becomes negligible and the donor luminosity dominates, making the tracks essentially coincident. After point D the absence of any contact phase prevents the occurrence of bright X-ray emission as only a very weak WFA stage is possible. Therefore, after point D the two tracks coincide. For illustrative purposes alone, in order to show the maximum contribution induced by X-ray irradiation, we assume that all the donor wind is somehow accreted. So, the second track in Fig. 3 and 4 accounts for X-ray illumination also after point D1.

5 PROPERTIES OF THE ULX COUNTERPARTS

The calculations presented in the previous Section can be used to constrain the properties of the donor stars in ULX systems by comparing their position on the HR or CM diagrams with the evolutionary tracks of massive BH binaries. This approach may actually provide interesting clues also on the properties of the binary system itself, including the BH mass.

5.1 Case A mass transfer

In Figures 5 and 6 we show the position in the CM diagram of the proposed counterparts of the four ULXs consid-

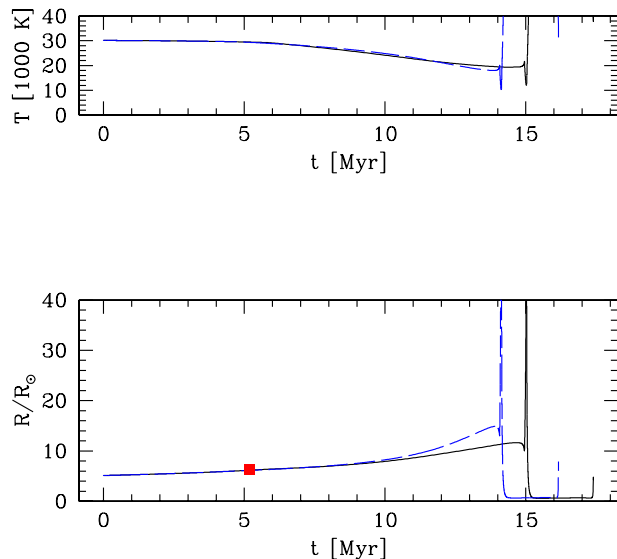


Figure 2. Evolution of surface temperature and radius for a $15M_{\odot}$ donor around a $10M_{\odot}$ (black-solid line) and a $100M_{\odot}$ (blue-dashed line) black hole. The red square marks the onset of the contact phase during MS. The two binaries have the same parameters of those shown in Figure 1. We note that the lifetime of a donor undergoing a case A mass transfer is slightly longer than the MS lifetime of the corresponding single star ($10^6 - 10^7$ yrs) because the nuclear burning timescale is slightly increased as a consequence of the mass lost during mass transfer.

ered, along with the evolutionary tracks of irradiated donor stars in binary systems undergoing a case A mass transfer with optical contamination from the disc. The tracks are plotted only during the contact phases (e.g. A-B, C-D) as only during these phases, the ULX is active. In the stellar mass BH case, we assume that the total isotropic luminosity is Eddington-limited. If the accretion rate becomes super-Eddington, we set $\dot{M} = \dot{M}_{Edd}$ and the excess mass is expelled from the system. We plotted for comparison also the track of a non-irradiated, single star of $15M_{\odot}$.

5.1.1 Differences between stellar BH and IMBH systems

Comparing Fig. 5 and 6 it is readily clear that, at corresponding stages, the V magnitude of an IMBH binary is smaller by ~ 0.5 mag (i.e. the luminosity higher by a factor ~ 1.5) than that of a stellar BH binary. The main reason for this difference stems from the larger contribution to the

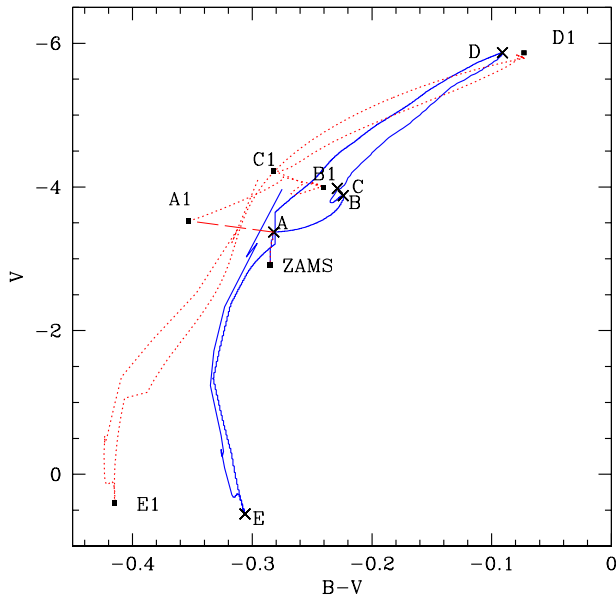


Figure 3. CM diagram for a $15 M_{\odot}$ donor accreting on a $10 M_{\odot}$ BH. The *blue-solid line* is the CM diagram for a non-irradiated star, while the *red-dotted line* takes into account both the X-ray irradiation of the stellar surface and the optical contribution of the accretion disc. The two tracks share the initial part of the curve (from ZAMS to point A), as no irradiation is present at this stage. Mass transfer sets in at point A. The contact phase ends in point B (and B1), very close to the terminal age main sequence. In point C (C1) the star is burning its H-shell and a new contact phase begins lasting up to point D (D1). In point E (E1) the star begins He core burning. After point D (D1) no other contact episodes occur throughout the evolution.

optical emission coming from the irradiated accretion disc around an IMBH and from the intrinsic larger luminosities of donors around IMBH (see Fig.1). Assuming a fixed orbital separation and a standard tidal truncation scenario with the accretion disc radius $R_D \sim 70\%R_L$, two binaries with mass ratios $q = 0.1$ and $q = 1$ have $R_{D,q=0.1}/R_{D,q=1} \sim 2$. Since for an IMBH binary $q \lesssim 0.1$, whereas a stellar BH binary has $q \sim 1$, disc contamination will always be larger in the IMBH case. Evolving a binary with a larger IMBH ($500M_{\odot}$), we found only second order differences with respect to the tracks of a binary with a $100M_{\odot}$ IMBH, as the Roche lobe radius is nearly the same.

A major difference between the stellar BH and IMBH concerns the possible presence of beamed emission. In order to emit apparent isotropic luminosities of $\lesssim 10^{40}$ erg s^{-1} without seriously violating the Eddington limit, a stellar mass BH binary must find a way to collimate its emission. For a beaming factor ~ 0.1 , both the disc and donor irradiation are strongly reduced as the X-rays can not intercept the outer disc and stellar surfaces. Then, the tracks on a CM diagram will be more similar to those of a non-irradiated system. However, as shown in Fig.3, the differences in the colors and magnitudes between an irradiated and a non-irradiated system during the contact phases are small (~ 0.1 mag for the stellar BH and ~ 0.2 mag for the IMBH case) and are

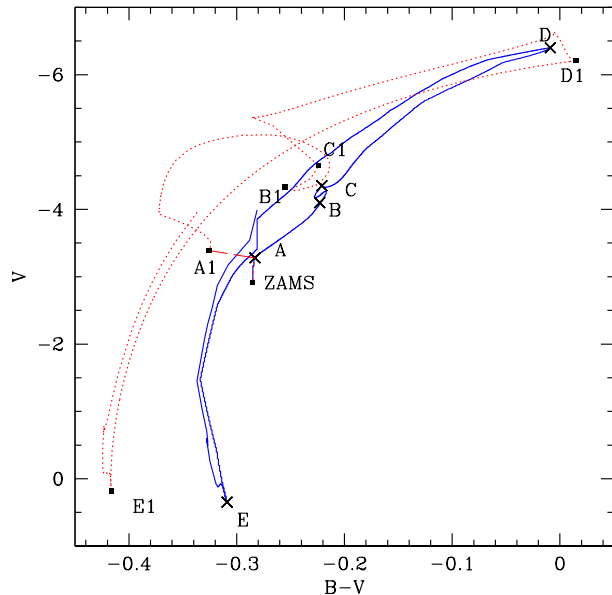


Figure 4. CM diagram for a $15 M_{\odot}$ donor accreting on a $100 M_{\odot}$ BH. The labels have the same meaning as in fig. 3. The irradiation has a stronger effect than in the stellar BH case, giving differences in magnitudes as high as 0.2 mag on the B-V scale during the main sequence.

therefore neglected considering the present photometric accuracy .

5.1.2 Optical identification

NGC4559 X-7: as can be seen from Figures 5 and 6, because of the turnoff occurring during the giant phase, the candidate counterparts of NGC4559 X-7 labeled 2, 3 and 4 can be immediately ruled out while, for a stellar mass BH, object 6 is consistent with the colors and luminosity of the least massive donor considered ($\sim 10M_{\odot}$). On the other hand, the point representing objects 1, 5 and 8 overlap the evolutionary tracks of stars in binaries with mass transfer. A MS star with a mass up to $50M_{\odot}$ is not consistent with the colors and luminosity of object 1, regardless of the BH mass. However, during the H-shell burning phase, a $\sim 50M_{\odot}$ star in a stellar mass BH system or a $\sim 30 - 50M_{\odot}$ star in an IMBH system turn out to be compatible with the photometric properties of object 1. Considering the other proposed counterparts, a MS star with a mass smaller than $15M_{\odot}$ around a stellar BH can not account for any of them as, at the end of the MS, the V band magnitude is too small. Object 5 can be well explained with a MS donor of $15-30M_{\odot}$ or a giant of $10-15M_{\odot}$.

NGC1313 X-2: considering the second contact phase in a stellar BH binary (beyond the starred symbol in Fig. 5), we find that a donor of $\sim 15M_{\odot}$ undergoing H-shell burning can account for the colors and magnitude of the candidate counterpart C1. In case of a IMBH binary, Fig. 6 shows that a $10-15M_{\odot}$ donor is consistent with the properties of object C1 both on the MS and during H-shell burning. On the other hand, object C2 can be firmly ruled out as possible counterpart of the ULX.

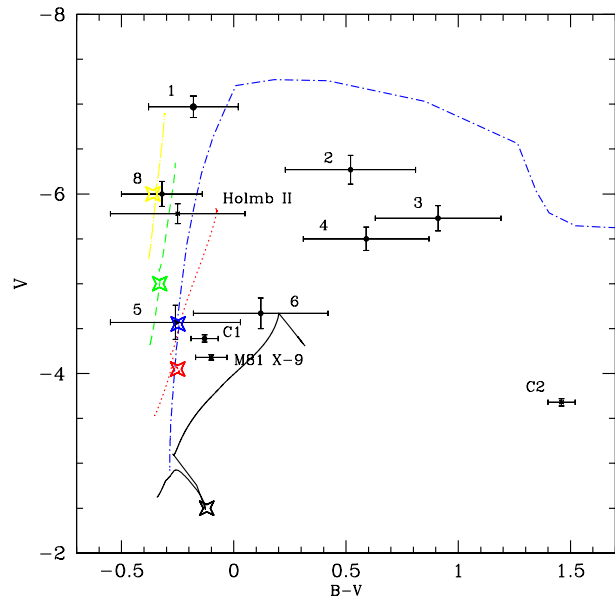


Figure 5. CM diagram for stars of 10, 15, 30 and $50M_{\odot}$ (black-solid, red-dotted, green-dashed, yellow-dot dashed line, respectively) starting mass transfer onto a $10M_{\odot}$ BH during MS (case A). The blue-dot dashed line is the track of a single non-irradiated $15M_{\odot}$, plotted for comparison. The crosses are the photometric points of the counterparts of NGC 4559 X-7 (1–6, 8), NGC 1313 X-2 (C1, C2), Holmberg II X-1 (Holm II) and M 81 X-9. The binary tracks are plotted only during the contact phases. The starred symbol denotes the point where the MS ends and H-shell burning sets in.

Holmberg II X-1: if the accretor is a stellar BH, then either a star with $15 < M < 30M_{\odot}$ during the H-shell burning phase or a donor with $\sim 50M_{\odot}$ on the MS can account for the observed photometric properties of the optical counterpart. For an IMBH system, the situation is similar, except that also a $10M_{\odot}$ donor is compatible when in the H-shell burning phase.

M81 X-9: the optical counterpart of this ULX is the faintest considered in this paper and is compatible only with a $< 15M_{\odot}$ donor during H-shell burning for a stellar BH or with a $\lesssim 10M_{\odot}$ donor on the MS or H-shell burning phase for an IMBH.

5.1.3 Mass transfer rate

In Figure 7 we show the mass transfer rate in binary systems undergoing a case A mass transfer onto a stellar BH of $10M_{\odot}$ or an IMBH of $100M_{\odot}$. The horizontal lines are the X-ray luminosities of the four ULXs reported in Table 1 and, as already discussed in §3, should be considered as lower limits for the bolometric luminosity of each source (which is estimated to be a factor ~ 2 higher; see Table 1). We note that these values are indicative as both the sources show a factor of a few variability and the measurements of the X-ray fluxes are usually affected by rather large errors.

In the **stellar BH case**, the mass transfer rate does not provide any further constraint as the relation between mass loss and luminosity becomes $L_{\text{bol}} = \dot{M}\eta c^2 b$ where b is the

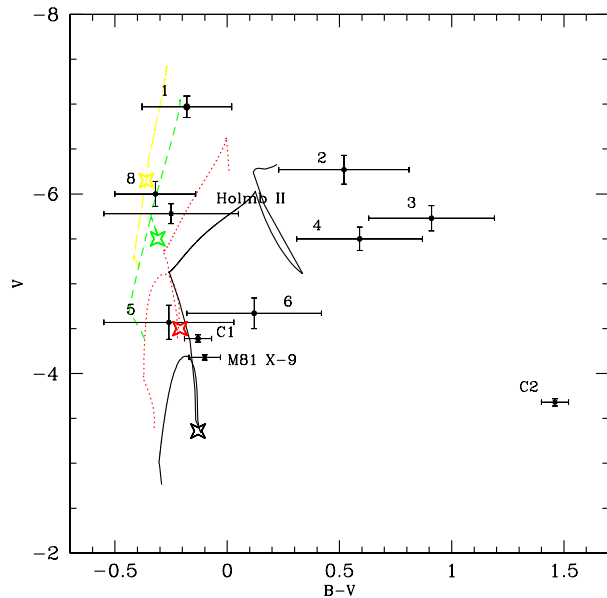


Figure 6. Same as Figure 5 for a BH of $100M_{\odot}$.

beaming factor whose value is unknown. In the present paper we are considering only standard geometrically thin and optically thick discs (Shakura-Sunyaev discs) and any genuine isotropic super-Eddington luminosity produced by alternative radiation-pressure dominated discs (e.g. Begelman 2002, Begelman 2006) will give a different optical contamination with respect to that calculated in the present work. In the **IMBH case**, the mass transfer rates are very similar to those of the stellar BH binaries. However we can further constrain the donor masses for NGC4559 X-7, as it is possible to rule out all the MS donors with $M \lesssim 30M_{\odot}$. For NGC1313 X-2 a $\sim 15M_{\odot}$ donor can give the required \dot{M} during a certain fraction of its MS lifetime. For Holmberg II X-1 no further constraints can be obtained, while for M81 X-9 it is possible to rule out the $10M_{\odot}$ MS donor, leaving as unique possibility a $10M_{\odot}$ donor in the H-shell burning phase.

In table 3 and 4 we show all the binaries compatible with the observed optical counterparts given the combined constraints coming from the mass transfer rate and the CM diagram.

5.2 Case B and C mass transfer

When the donor star starts a case B or C mass transfer, the evolution of the binary may be completely different with respect to what reported above. If the contact phase sets in at the beginning of the Hertzsprung Gap, when the donor radius is still relatively small (e.g. $P \lesssim 10$ days for a $15M_{\odot}$ donor), the contact phase is extremely short lived (a few 10^4 yrs) and \dot{M} can reach a few $10^{-5}M_{\odot} \text{ yr}^{-1}$ (in some cases up to $10^{-3}M_{\odot} \text{ yr}^{-1}$). The tracks on the CM diagram are similar to those calculated for case A, with a turnoff during the H-shell burning at the point where the system becomes detached. If the contact phase sets in at the end of the Hertzsprung Gap ($P \gtrsim 10$ days for a $15M_{\odot}$ donor) or later

Table 3. Consistent donor masses for case A mass transfer onto a $10M_{\odot}$ black hole. A 'X' (or the name of the donor when there are multiple optical counterparts for the same ULX) marks the entry corresponding to a certain donor mass and contact phase (MS or H-shell). Each donor must satisfy the condition that the track on the CM diagram crosses the optical counterpart.

	$10M_{\odot}$		$15M_{\odot}$		$30M_{\odot}$		$50M_{\odot}$	
	MS	H-shell	MS	H-shell	MS	H-shell	MS	H-shell
NGC4559 X-7		6		5	5	8	8	1
NGC1313 X-2				C1				
Holmberg II X-1				X		X	X	
M81 X-9		X						

Table 4. As Table 3 but for a $100M_{\odot}$ IMBH and with the further constraint on the mass transfer rate. Each donor in the table has a mass transfer rate high enough to reach at least the observed X-ray luminosity assuming isotropic emission.

	$10M_{\odot}$		$15M_{\odot}$		$30M_{\odot}$		$50M_{\odot}$	
	MS	H-shell	MS	H-shell	MS	H-shell	MS	H-shell
NGC4559 X-7		5		5,8		1,8	8	1
NGC1313 X-2		C1	C1	C1				
Holmberg II X-1		X		X		X	X	
M81 X-9		X						

(case C mass transfer), \dot{M} is comparable to that of a case A mass transfer binary during H-shell burning, but now the donor enters the region of the single giant stars on the CM diagram and the differences with the case A tracks become sharp.

In this situation all the previously excluded optical counterparts of NGC4559 X-7 (objects 2, 3 and 4) become good candidates, while objects 1, 5, 6 and 8 are ruled out. In the case of NGC 1313 X-2, both counterparts can be excluded. In particular, object C2 can be definitively ruled out as its position is not consistent with any irradiated or non-irradiated track. Also the counterparts of Holmberg II X-1 and M81 X-9 are not consistent with any case B or C binary system. Finally, the most massive donors ($M \geq 30M_{\odot}$) are too bright at this stage to be proposed as candidate counterparts regardless of the compact object mass.

6 DISCUSSION AND CONCLUSIONS

In this paper we have shown that the effects of the binary evolution on the optical properties of a donor star in a ULX binary system can significantly alter its colors and evolution. We included also the contribution of the optical emission of the accretion disc and the X-ray irradiation of the donor and disc surfaces. The evolutionary track of a donor in an accreting binary on the CM diagram is very different with respect to that of a single isolated star. These important differences can not be overlooked when trying to identify the donor mass of a ULX. We calculated tracks for stellar and intermediate mass black holes, and demonstrate the brighter nature of the IMBH as an intrinsic phenomenon produced by the low mass ratio in the binary.

The photometric data of four ULX counterparts have been compared with the evolutionary tracks of massive

donors on the CM diagram. We find that the counterparts 2, 3 and 4 of NGC 4559 X-7 are consistent only with donors of $10\text{--}15M_{\odot}$ undergoing a case B or C mass transfer episode. The only possibility for objects 5 and 8 is a very massive ($\sim 50M_{\odot}$) MS donor or a H-shell burning donor with mass between $10\text{--}15$ and $30M_{\odot}$. Finally, object 1 is compatible only with a very massive ($M \gtrsim 50M_{\odot}$) donor in a H-shell burning phase. Our results are quite different with respect to what obtained in previous analysis. Soria et al. (2005) compared theoretical evolutionary tracks of single stars between 9 and $25M_{\odot}$ with the position in the CM diagram of the counterparts of NGC4559 X-7. They find that the colors and luminosity of six out of seven stars are consistent with the tracks of main sequence, blue or red supergiant with masses in the range $10\text{--}15 M_{\odot}$ and ages ~ 20 Myr. Their favored counterpart, object 1, was identified with a main sequence or blue supergiant of $\sim 20M_{\odot}$ and an age of ~ 10 Myr, although Soria et al. (2005) recognize that X-ray irradiation may affect its colors and hence its classification. Irradiation effects were taken into account by Copperwheat et al. (2007), giving a donor mass of $5\text{--}20M_{\odot}$ for object 1. In their work, however, Copperwheat et al. (2007) considered irradiation on single stars and did not take into account the effects of the markedly different evolution of a donor star in a binary system.

As far as NGC1313 X-2 is concerned, we definitely rule out the candidate counterpart C2 and identify C1 as a H-shell burning donor of $10M_{\odot} < M < 15M_{\odot}$ around a stellar mass black hole or a $\lesssim 15M_{\odot}$ donor undergoing RLOF during MS (or the H-shell burning phase) in an IMBH binary system. On statistical grounds alone, it is then more likely that NGC1313 X-2 hosts a $\sim 100M_{\odot}$ BH rather than a stellar mass BH as the H-shell burning phase is much shorter than the MS phase. Our result for object C2 leaves only C1

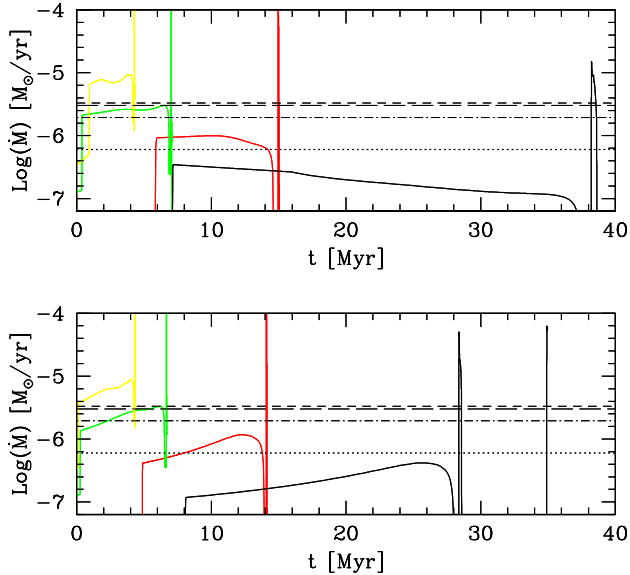


Figure 7. Mass transfer rate of 10, 15, 30 and $50M_{\odot}$ donors around a $10M_{\odot}$ stellar BH (*upper panel*) and $100M_{\odot}$ IMBH (*bottom panel*) undergoing a case A mass transfer. The mean mass transfer rate required to produce the X-ray luminosities reported in Table 1 is indicated with a *dotted* (NGC1313 X-2) *dot-dashed* (M81 X-9), *long dashed* (Holmberg II) and *short dashed* (NGC4559 X-7) line. The adopted efficiency of conversion of gravitational potential energy into radiation is $\eta = 0.1$.

as the likely counterpart of NGC 1313 X-2, in agreement with the evidence coming from the refined X-ray astrometry of the field recently reported by Liu et al. (2007). On the basis of single star isochrone fitting of the parent stellar population, Pakull, Grisé & Motch (2006) and Ramsey et al. (2006) estimate a maximum MS mass of $8-9M_{\odot}$ for object C1. Liu et al. (2007) find consistency with either a $\sim 8M_{\odot}$ star of very low metallicity or an O spectral type, solar metallicity star of $\sim 30M_{\odot}$. Our estimated range of donor masses for object C1 appears more in agreement with the value ($10-18M_{\odot}$) reported by Mucciarelli et al. (2007), probably because they also included the contribution of the disc and irradiation effects. In Holmberg II X-1 there are several possibilities, and we can only rule out stars with $M < 10M_{\odot}$ (Copperwheat et al. 2007 give a lower bound of $5M_{\odot}$), while for M81 X-9 we are left with the unique possibility that the donor is a $\sim 10M_{\odot}$ star in the H-shell burning phase.

We conclude therefore that in all previous work where the binary evolution and/or irradiation effects were not taken into account, the donor mass has been systematically overestimated. We find that mass transfer occurring at late stages is very unlikely, not only for the short timescale of the contact phase (10^3-10^5 yrs) but also for the incompatibility of the optical colors with the majority of the observed counterparts. If mass transfer sets in during MS, two contact phases occur (segments A-B and C-D). The mass transfer timescales are $t_{A-B} \sim 10^6-10^7$ yrs and $t_{C-D} \sim 10^3-10^5$ yrs (depending on the donor mass). Therefore assuming a flat distribution of periods between 1 and ~ 10 days, as during MS the contact phase is reached for $P_{orb} \lesssim 2$ days, we ex-

pect a factor $\sim \frac{10}{2} \times \frac{t_{A-B}}{t_{C-D}} \simeq 500-5000$ more main sequence systems than H-shell burning donors.

7 ACKNOWLEDGEMENTS

We would like to thank Onno Pols and Jasinta Dewi for the kind support in the use of the Eggleton code, and Simon Portegies Zwart, Monica Colpi and Manfred Pakull for useful discussions. We also thank the referee of a previously submitted version of this work for his valuable comments that helped to improve our paper.

REFERENCES

- Abel, T., Bryan, G. L., & Norman, M. L. 2000, *ApJ*, 540, 39
- Alexander, T. & Livio, M. 2004, *ApJ*, 606, L21
- Arp, H., Gutiérrez C.M., & López-Corredoira M. 2004, *A&A*418, 877
- Ayal, S., Livio, M. & Piran, T. 2000, *ApJ*, 545, 772
- Baumgardt, H., Makino, J., & Ebisuzaki, T. 2004, *ApJ*, 613, 1143
- Baumgardt, H., Hopman, C., Portegies Zwart, S., & Makino, J. 2006, *MNRAS*, 372, 467
- Begelman, M.C. 2002, *ApJ*, 568, L97
- Begelman, M. C. 2006, *ApJ*, 643, 1065
- Blecha, L., Ivanova, N., Kalogera, V., Belczynski, K., Fregeau, J., & Rasio, F. 2006, *ApJ*, 642, 427
- Clark, D. M., et al. 2005, *ApJ*, 631, L109
- Colbert, E. J. M., & Ptak, A. F. 2002, *ApJS*, 143, 25
- Copperwheat, C., Cropper, M., Soria, R., & Wu, K. 2005, *MNRAS*, 362, 79
- Copperwheat, C., Cropper, M., Soria, R., & Wu, K. 2007, *MNRAS*, 376, 1407
- Cropper, M., Soria, R., Mushotzky, R. F., Wu, K., Markwardt, C. B. & Pakull, M. 2004, *MNRAS*, 349, 39
- de Jager, C., Nieuwenhuijzen, H., & van der Hucht, K. A. 1988, *AAPS*, 72, 259
- de Jong, J.A., van Paradijs, J., & Augusteijn, T. 1996, *A&A*, 314, 484
- Demircan, O. & Kahraman, G. 1991, *ApSS*, 181, 313
- Dewangan, G. C., Miyaji, T., Griffiths, R. E. & Lehmann, I. 2004, *ApJ*, 608, L57
- Dewangan, G. C., Griffiths, R. E., Choudhury, M., Miyaji, T., & Schurch, N. J. 2005, *ApJ*, 635, 198
- Dubus, G., Lasota, J., Hameury, J. & Charles, P. 1999, *MNRAS*, 303, 139
- Ebisawa, K., Życki, P., Kubota, A., Mizuno, T. & Watarai, K. 2003, *ApJ*, 597, 780
- Eggleton, P. P. 1971, *MNRAS*, 151, 351
- Eggleton, P. P. 1983, *ApJ*, 268, 368
- Eggleton, P. P., Tout, C. A. & Fitchett, M. J. 1989, *ApJ*, 347, 998
- Feng, H., & Kaaret, P. 2006, *ApJ*, 650, L75
- Feng, H., & Kaaret, P. 2007, *ArXiv e-prints*, 706, arXiv:0706.3233
- Fiorito, R., & Titarchuk, L. 2004, *ApJ*, 614, L113
- Frank, J., King, A.R., & Raine, D.J. 2002, *Accretion Power in Astrophysics* (Cambridge University Press)
- Gierliński, M. & Done, C. 2004, *MNRAS*, 347, 885

- Gioia, I. M., Maccacaro, T., Schild, R. E., Wolter, A., Stocke, J. T., Morris, S. L., & Henry, J. P. 1990, *ApJS*, 72, 567
- Goad, M. R., Roberts, T. P., Knigge, C., & Lira, P. 2002, *MNRAS*, 335, L67
- Goad, M. R., Roberts, T. P., Reeves, J. N., & Uttley, P. 2006, *MNRAS*, 365, 191
- Gonçalves, A. C., & Soria, R. 2006, *MNRAS*, 371, 673
- Gürkan, M. A., Freitag, M., & Rasio, F. A. 2004, *ApJ*, 604, 632
- Gutiérrez, C. M., & López-Corredoira, M. 2005, *ApJ*, 622, L89
- Hopman, C., Portegies Zwart, S. F. & Alexander, T. 2004, *ApJ*, 604, L101
- Howarth, I. D. & Prinja, R. K. 1989, *ApJS*, 69, 527
- Irwin, J. A., Bregman, J. N. & Athey, A. E. 2004, *ApJ*, 601, L143
- Jeltema, T. E., Canizares, C. R., Buote, D. A. & Garmire, G. P. 2003, *ApJ*, 585, 756
- Kaaret, P., Ward, M. J. & Zezas, A. 2004, *MNRAS*, 351, L83
- Kaaret, P. 2005, *ApJ*, 629, 233
- Kalogera, V., King, A. R. & Rasio, F. A. 2004, *ApJ*, 601, L171
- King, A. R., Davies, M. B., Ward, M. J., Fabbiano, G. & Elvis, M. 2001, *ApJ*, 552, L109
- King, A. R., & Dehnen, W. 2005, *MNRAS*, 357, 275
- Körding, E., Falcke, H. & Markoff, S. 2002, *A&A*, 382, L13
- Lamers, H. J. G. L. M. & Leitherer, C. 1993, *ApJ*, 412, 771
- Landau, L. D., & Lifshitz, E. M. 1975, *The classical theory of fields* (Pergamon press, 4th rev.engl.ed)
- Liu, J.-F., & Bregman, J. N. 2005, *ApJS*, 157, 59
- Liu, J.-F., Bregman, J. N., & Seitzer, P. 2002, *ApJ*, 580, L31
- Liu, J.-F., Bregman, J. N., & Seitzer, P. 2004, *ApJ*, 602, 249
- Liu, J.-F., Bregman, J., Miller, J., & Kaaret, P. 2007, *ApJ*, 661, 165
- Madau, P., & Rees, M. J. 2001, *ApJ*, 551, L2
- Madhusudhan, N. et al. 2006, *ApJ*, 640, 918
- Miller, J. M., Fabbiano, G., Miller, M. C. & Fabian, A. C. 2003, *ApJ*, 585, L37
- Miller, J. M., Fabian, A. C. & Miller, M. C. 2004, *ApJ*, 607, 931
- Mucciarelli, P., Zampieri, L., Falomo, R., Turolla, R., & Treves, A. 2005, *ApJ*, 633, L101
- Mucciarelli, P., Casella, P., Belloni, T., Zampieri, L., & Ranalli, P. 2006, *MNRAS*, 365, 1123
- Mucciarelli, P., Zampieri, L., Treves, A., Turolla, R., & Falomo, R. 2007, *ApJ*, 658, 999
- Pakull, M. & Mirioni, L. 2002, *astroph/0202488*
- Pakull, M.W., Grisé, F., & Motch, C. 2006, *IAUS*, 230, 293
- Patruno, A., Colpi, M., Faulkner, A., & Possenti, A. 2005, *MNRAS*, 364, 344
- Podsiadlowski, P., Rappaport, S., & Pfahl, E. D. 2002, *ApJ*, 565, 1107
- Podsiadlowski, P., Rappaport, S., & Han, Z. 2003, *MNRAS*, 341, 385
- Pols, O. R., Tout, C. A., Eggleton, P. P., & Han, Z. 1995, *MNRAS*, 274, 964
- Pols, O. R., Schroder, K.-P., Hurley, J. R., Tout, C. A., & Eggleton, P. P. 1998, *MNRAS*, 298, 525
- Portegies Zwart, S. F., Baumgardt, H., Hut, P., Makino, J., & McMillan, S. L. W. 2004, *Nat*, 428, 724
- Portegies Zwart, S. F., Dewi, J. & Maccarone, T. 2004, *MNRAS*, 355, 413
- Ramsey, C. J., Williams, R. M., Gruendl, R. A., Chen, C.-H. R., Chu, Y.-H., & Wang, Q. D. 2006, *ApJ*, 641, 241
- Rappaport, S. A., Podsiadlowski, P., & Pfahl, E. 2005, *MNRAS*, 356, 401
- Rees, M. J. 1988, *Nat*, 333, 523
- Roberts, T. P., Goad, M. R., Ward, M. J., Warwick, R. S., O'Brien, P. T., Lira, P., & Hands, A. D. P. 2001, *MNRAS*, 325, L7
- Roberts, T. P., Goad, M. R., Ward, M. J. & Warwick, R. S. 2003, *MNRAS*, 342, 709
- Roberts, T. P., Warwick, R. S., Ward, M. J., Goad, M. R., & Jenkins, L. P. 2005, *MNRAS*, 357, 1363
- Shakura, N. I. & Sunyaev, R. A. 1973, *A&A*, 24, 337
- Shimura, T. & Takahara, F. 1995, *ApJ*, 445, 780
- Soberman, G. E., Phinney, E. S. & van den Heuvel, E. P. J. 1997, *A&A*, 327, 620
- Soria, R., Cropper, M., Pakull, M., Mushotzky, R. & Wu, K. 2005, *MNRAS*, 356, 12
- Soria, R. & Motch, C. 2004, *A&A*, 422, 915
- Stobbart, A.-M., Roberts, T. P., & Wilms, J. 2006, *MNRAS*, 368, 397
- Strohmayer, T. E., & Mushotzky, R. F. 2003, *ApJ*, 586, L61
- Strohmayer, T. E., Mushotzky, R. F., Winter, L., Soria, R., Uttley, P., & Cropper, M. 2007, *ApJ*, 660, 580
- Swartz, D. A., Ghosh, K. K., McCollough, M. L., Pannuti, T. G., Tennant, A. F. & Wu, K. 2003, *ApJS*, 144, 213
- Swartz, D. A., Ghosh, K. K., Tennant, A. F. & Wu, K. 2004, *ApJS*, 154, 519
- Tully, R. B. 1988, *Science*, 242, 310
- Ulmer, A. 1999, *ApJ*, 514, 180
- van Paradijs, J., & McClintock, J. E. 1994, *A&A*, 290, 133
- Watarai, K., Mizuno, T. & Mineshige, S. 2001, *ApJ*, 549, L77
- Zampieri, L., Mucciarelli, P., Falomo, R., Kaaret, P., Di Stefano, R., Turolla, R., Chierigato, M. & Treves, A. 2004, *ApJ*, 603, 523
- Zampieri, L., Turolla, R. & Szuszkiewicz, E. 2001, *MNRAS*, 325, 1266
- Zezas, A., Fabbiano, G., Rots, A. H. & Murray, S. S. 2002, *ApJ*, 577, 710